Boron spectral density and disorder broadening in B-doped diamond

K.-W. Lee and W. E. Pickett
Department of Physics, University of California, Davis, California 95616, USA
(Received 14 September 2005; revised manuscript received 7 December 2005; published 6 February 2006)

Comparison of periodic B dopants with a random alloy of substitional boron in diamond is carried out using several supercells and the coherent potential approximation (CPA) for the random alloy case. The main peak in the B local density of states is shifted to lower binding energy compared to the corresponding C peak in intrinsic diamond. In supercells, this shows up as strongly B-character bands split from bulk C bands away from the zone center, in an energy region around −1 eV. Even for a $4\times4\times4$ supercell (BC_{127}), effects of the dopant order are evident in the form of primarily B-character bands just below the Fermi level at the supercell zone boundary. The bands resulting from the CPA are of continuous mixed C-B character. They resemble virtual crystal bands, but broadened somewhat reflecting the disorder-induced lifetime, and are consistent with angle-resolved photoemission band maps. The B character is 1.7 times larger than for C (per atom) near the top of the valence bands for CPA, and roughly the same for supercells. CPA results are particularly useful since they characterize the wave vector and energy dependence of disorder broadening.

DOI: 10.1103/PhysRevB.73.075105 PACS number(s): 71.20.Be, 71.55.Cn, 74.70.Ad

I. INTRODUCTION

The discovery and confirmation of superconductivity in diamond heavily doped with boron[1–6] has provoked interest in the mechanism and character of the pairing that is responsible. There are several confirmations of superconductivity around 4 K for 2–3 % doping, and a recent report[5] indicates $T_c \approx 11.5$ K for 4.7% boron concentration in homoepitaxial films. While the picture of 3% hole-doped diamond as a degenerate metal has been the most common assumption,[7–12] there has also been the possibility that the boron acceptor level is too deep for itinerant conductivity to arise, leading to a picture of a nondegenerate doped semiconductor[13] with possible correlated behavior.[14] An angle-resolved photoemission spectroscopy (ARPES) study[15] on heavily B-doped diamond has found the Fermi level to lie a few tenths of an eV within the valence bands, establishing the degenerate-metal picture as the correct one for this system.

It is useful to review briefly the history of B doping of diamond. Although it has been clear for decades that B is responsible for the color of blue diamonds, and the desire for *p*-type semiconducting diamond has been intense for some time, the existing information about the isolated B acceptor is sketchy. The energy of the acceptor level is agreed to be $E_B = 0.37$ eV.[16] This binding energy is too large for this impurity to be treated accurately at the effective mass level, hence its wave function is not as greatly extended as that of a shallow level would be. On the other hand, this is not truly a deep level (since E_B is only 7% of the band gap) in which the defect state extends over only a shell or two of neighboring C atoms.

The existing theoretical studies aimed at gleaning information about the B acceptor state are not very conclusive. Finite clusters (up to 59 atoms) were used by Mainwood,[17] who obtained for substitutional B a threefold degenerate, mainly B $2p$, state 0.36 eV above the uppermost occupied diamond valence state. The cluster was allowed to relax, with the B-C bonds increasing by 10% (0.15Å), a much larger amount than has been obtained in more recent calculations. The very limited cluster size, with its surface effects, does not allow for clear conclusions. Barnard *et al.* reported some results from 64 atoms (periodic) supercells,[18] but as we show here for a larger supercell, the local density approximation (LDA) does not produce a gap acceptor state at such densities (∼1%). A tight-binding total energy method was used by Sitch *et al.*, who reported only atomic relaxation using a 216-atom supercell.[19] C atoms neighboring the substitutional B relaxed outward by 4% (bond length of 1.60Å). Their study was focused instead on doping of amorphous carbon.

Adopting the ARPES demonstration[15] that the Fermi level lies within the itinerant valence bands, there are a few choices to be made in describing the electronic structure, and the subsequent evaluation of the character and strength of the electron-phonon (EP) coupling is determined to some extent by this choice. The published studies of superconductivity in B-doped diamond concur that EP coupling provide the pairing mechanism, in spite of applying different approximations to achieve their separate estimates. We briefly describe the various approaches.

Three groups have adopted the virtual crystal approximation (VCA), making use of the fact that B is chemically and physically similar to C, especially when they share a common environment; in this case each is surrounded by C atoms on a diamond lattice. In such cases, the itinerant wavefunctions average over the B and C atoms and replacing each nucleus by an average charge constitutes the VCA. Adopting the VCA, Boeri, Kortus, and Andersen[7] then applied linear response theory for harmonic phonons and calculated the phonon frequencies at ∼50 q points. This allowed the evaluation of the EP spectral function and strength of coupling. Lee and Pickett[8] also adopted the VCA for the underlying electronic structure. As suggested by the analogy with MgB_2 where holes are doped into strong covalent bonds, they found a very large EP matrix element for the bond-stretch mode and, making use of the small Fermi surfaces, assumed it varied slowly with wave vector q up to $2k_F$ (k_F is the Fermi

wave vector). They calculated by the frozen phonon method the phonon renormalization of the bond-stretch mode by the doped carriers, and from two related but separate directions arrived at the EP coupling strength. Also adopting the VCA viewpoint, Ma *et al.*[11] used methods very similar to those of Boeri *et al.* (but different codes) and the same phonon mesh, but studied electron doping as well as hole doping.

Blase, Adessi, and Connétable[9] and Xiang *et al.*,[10] on the other hand, used a supercell approach in which the B dopants keep their chemical identity (actual B atoms), but to apply standard solid state methods the dopant atoms had to be repeated periodically. This supercell approach restricts dopant concentrations to certain commensurate fractions but this is no real limitation because B concentrations are only known approximately. Blase *et al.* calculated phonons and EP coupling only at $q=0$ in a 54-atom (BC_{53}) supercell and estimated the coupling strength accordingly. Xiang *et al.* treated both 16-atom and 36-atom supercells, using phonons at a few q points.

Naturally the various calculations contain differences in detail and in general it is not possible to compare several of the intermediate results. Both groups using the supercell approach have suggested that there are aspects of their results that make the supercell approach superior, or perhaps necessary. On the other hand, the ARPES data[15] lead to band dispersions very much like the diamond (or VCA) bands, perhaps broadened by disorder.

There is another approach to the treatment of randomly positioned dopant atoms, the coherent potential approximation (CPA). The CPA allows the dopant to retain its identity, but produces an effective medium that accounts for random disorder. The CPA method has not been applied to evaluate the EP coupling in B-doped diamond, which is possible in principle, because linear response theory for phonons has not yet been incorporated into CPA codes. It is straightforward however to calculate the CPA electronic structure of B-doped diamond and compare results with the VCA and supercell approaches. In this paper we study in Sec. III selected supercells, and then provide CPA results (Sec. IV) for dilute B in diamond and make some comparisons both to supercell results and the VCA bands (which are hardly distinguishable from the diamond bands for small B concentrations). Using supercells we can study effects due to B-B interaction, and quantify specific effects that arise because of the periodicity that is imposed. It is also easy when using the supercell approach to evaluate the effect of B on the various shells of C neighbors. The CPA accounts for random positioning of the dopants and also allows the evaluation of disorder broadening of the bands (Sec. IV). We make a few observations about relaxation around a substitutional B atoms (Sec. V) which is not included in either the VCA or CPA method, and in Sec. VI provide a summary of the implications of our results.

II. STRUCTURE AND CALCULATION METHOD

The bulk diamond bond length is $d_{C\text{-}C}=1.54$ Å. For a substitutional B atom, the B-C bond length is increased by 2% and the neighboring C-C bond length is decreased by 1.3% in a LDA calculation with $3\times3\times3$ fcc primitive cell (BC_{53}).[9]

We have carried out calculations of "ordered impurities" using several supercells and of "randomly disordered impurities" using the CPA method, both of them with the full-potential nonorthogonal local-orbital minimum-basis scheme (FPLO).[20] The coherent potential approximation (CPA) method[21] implemented in FPLO is based on the Blackman-Esterling-Berk theory[22] that includes random off-diagonal matrix elements in the local orbital representation. Koepernik *et al.* provide a discussion of how randomness is treated in this atomic-orbital-based procedure.[21]

We have used three types of supercells: a large symmetric cell, a doubled cubic cell only in a (001) plane and a set of layered cells. A $4\times4\times4$ fcc primitive cell (BC_{127}) was used as a symmetric cell and $2\times2\times1$ cubic cell (BC_{31}) also was studied. The latter ($\approx3\%$ doping) is very close to the initally reported 2.5% doping superconductor. In addition, we used several supercells [$(1\times1\times2(BC_{15})$ to $1\times1\times5(BC_{39})$] layered in the c direction, which illustrated some systematic variations. The low level of B doping requires a sufficiently fine k point grid to sample the few unoccupied valence states that arise. Because of the different size of each Brillouin zone (BZ), k points used are different from each other, but we have used from 245 to 1000 k points in the irreducible wedge of each BZ, except for $4\times4\times4$ supercell. For the $4\times4\times4$ supercell, three irreducible k points should be enough to understand the band structure. However, the CPA requires a much finer k mesh to sample the wavevector and energy dependent spectral function, so 2045 k points were used in the irreducible wedge. For all calculations, valence orbitals for the basis set contained $1s2s2p3d$ for B and C.

III. ORDERED IMPURITIES (SUPERCELLS)

A. 2×2×1 (32-atom) supercell

First we address the supercell having a B concentration ($c_B\sim3\%$) very close to the initially reported superconducting concentration ($\sim2.5\%$). The upper portion of the valence band structures of the $2\times2\times1$ supercell is compared with that of intrinsic diamond in the top panel of Fig. 1. For better comparison, the bands of intrinsic diamond are raised by the Fermi energy (E_F) difference from the doped diamond so that the bands are aligned at the valence band maximum (VBM). B doping has three separate effects that are common to all of the supercells: (1) lowering E_F owing to hole doping (opposite direction[23] to the effect of C doping in $Mg(B_{1-x}C_x)_2$), (2) band splittings at the high-symmetry points in the BZ reflecting symmetry breaking, and (3) band shifts reflecting the difference in the B and C potentials.

The largest effect of the B doping occurs 1–2 eV below the Fermi level, which is easily seen on the $k_z=\pi/a$ plane (Z-R-A-Z lines in Fig. 1). Three bands along these lines are raised in energy by more than 1 eV by the addition of boron; the strong B character of these displaced bands is illustrated in the bottom panel of Fig. 1, where the "fatband" representation emphasizing B character is presented. These rather flat bands are strongly hybridized with the nearest neighbor (nn)

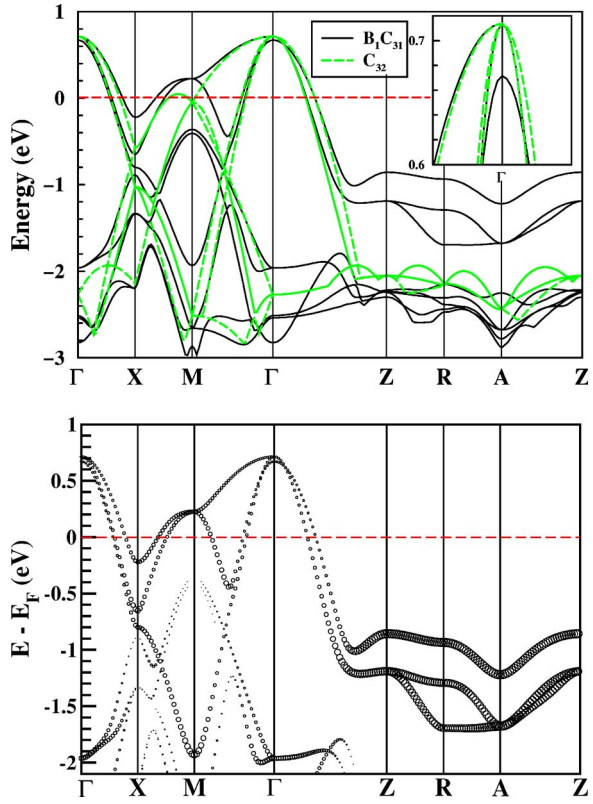

FIG. 1. (Color online) Top panel: Upper portion of the valence band structures of the $2\times2\times1$ supercell for the B-doped (BC_{31}) and intrinsic diamond (C_{32}). The bands are aligned at the top of the valence band. inset: Blowup of the band splitting by 42 meV along the M-Γ-Z lines due to the asymmetry of the supercell. Bottom panel: "Fatband" representation of the B $2p$ character. The main character is located in the range of -1.7 and -0.7 eV, a regime largely shifted by the B doping, on the $k_z=\pi/a$ plane. The symbol size is proportional to the B $2p$ character. The dashed horizontal line indicates the Fermi energy of BC_{31}. The symmetry points are given such as $(0,0,\xi)$ for $\Gamma(Z)$, $(0,1/2,\xi)$ for $X(R)$, and $(1/2,1/2,\xi)$ for $M(A)$. ξ is zero for the first symbols and 1 for the symbols in parentheses; units are π/a.

C $2p$ states, which provide about one-third of the band character. At the VBM which is threefold degenerate in intrinsic diamond, the B character and the *nn* C $2p$ character are also strongly mixed. Besides the mixing, the top of the valence bands at the Γ point in the B-doped diamond shows a tiny band splitting of 42 meV, as shown in inset of the top panel of Fig. 1. The origin of the splitting is not clear but its value is probably specific to this supercell.

The corresponding atom-projected density of states (DOS) is given in Fig. 2. As expected from the strong local B-C mixing, the B DOS resembles that of the *nn* C DOS. More specifically, however, the B and *nn* C are enhanced at the VBM. Their spectral densities show differences: the B DOS has much sharper peaks around -1 eV while that of the *nn* C continues more strongly to -4 to -6 eV. To summarize, the weights of the DOSs are arranged in the order of B, *nn* C, second neighbor ($2n$) C, and bulk C, in order of increasing binding energy.[24] This trend is consistent with the interpretation of x-ray absorption and emission spectroscopy by Nakamura *et al.*[25,26]

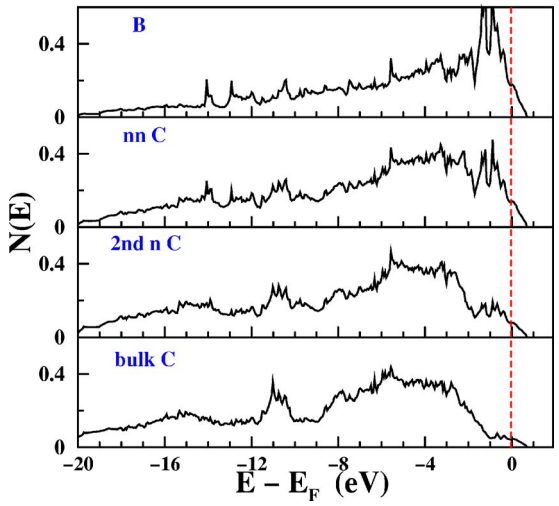

FIG. 2. (Color online) Atom-projected DOS for B and and three C neighbors in the $2\times2\times1$ supercell (BC_{31}). The B DOS is very similar to that of the *nn* C. Note the sharp peaks confined to B and the *nn* C atom between -2 and -1 eV, arising from strong B $2p$ character on the plane of $k_z=\pi/a$. For C atoms progressively further from the B atom, the peak at -11 eV becomes sharper. The B DOS is clearly shifted higher (to lower binding energy) compared to that of carbon.

B. 4×4×4 (128-atom) supercell

As large a supercell calculation as possible is desirable to extract information about the isolated B impurity. We first study the change in the band structure, keeping in mind that it reflects the periodic arrangement of the 0.8% concentration of B substitutionals in this supercell. The symmetry is such that the threefold degeneracy of the VBM is not split. The effective masses are changed very little, but we have not tried to identify possible changes in masses at the 1% level. Splitting of degeneracies by 0.3–0.4 eV can be seen at various places in the bands in Fig. 3: along Γ-X and at L near -0.2 eV. There are larger splittings (at L, for example) at energies below -1 eV in Fig. 3. At the Γ point, the cluster of degenerate bands at -1.3 eV in intrinsic diamond (coming

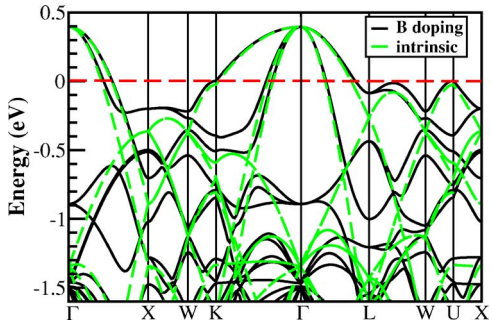

FIG. 3. (Color online) Upper portion of the valence band structures of $4\times4\times4$ supercell for the B doped (BC_{127}) and intrinsic diamond (C_{128}). At the symmetry points, the band splittings are obvious, especially at the Γ, X, and L points. The symmetry points follow the conventional notation for fcc BZ. (L denotes the zone boundary point in $\langle111\rangle$ direction.) The dashed horizontal line indicates E_F of the B-doped diamond.

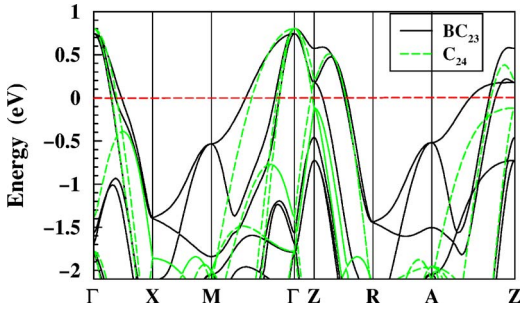

FIG. 4. (Color online) Upper portion of the valence band structures of the $1\times1\times3$ supercell for the B-doped (BC_{23}) and intrinsic diamond (C_{24}). This figure shows clearly the different origins of the band splittings at Γ and at Z. The dashed horizontal line indicates E_F of the B-doped diamond.

from zone folding) are split and shifted considerably by B addition. The threefold degenerate bands at −0.9 eV, having strong B character, have been raised by 0.5 eV, while others are shifted little. Thus even this large supercell shows effects of the periodicity of B atoms that will not be present if B atoms are distributed randomly. These effects are most evident when they produce new pieces of Fermi surface related specifically to the artificial periodicity, as is beginning to be the case in Fig. 3 along the *L*-*W* line. A higher doping level than the 0.8% of this supercell could lead to inaccuracies in properties determined by the Fermi surface, such as the electron-phonon spectral function.

C. Layered supercells

A set of layered supercells was studied to observe closely the asymmetry, changes in doping concentration, and effect of increasing the separation of the B atoms. Although the doped B concentration (2.5–6.25 %) varies in the each calculation, the band structures show considerable similarities. The upper portion of the valence band structures of the $1\times1\times3$ supercell is shown in Fig. 4. Bands of strong B $2p$ character are pushed upward into the −1.5 to −0.5 eV range along the *X*-*M* and *R*-*A* lines. This is the same energy range where *B* character is "pushed" in the other supercells.

The total DOS of the $(1,1,m)$ cubic supercells (m=2,3,4,5), corresponding to x=0.0625, 0.0417, 0.0313, and 0.025, are presented in Fig. 5 and show an interesting trend. As indicated by the arrows, decreasing x leads to a sharp peak at −1.6 eV and enhancement around 0.4 eV. With decreasing x, the lowest of the bands shown in Fig. 4 along the *X*-*M* line becomes flatter, resulting in enlargement of the peak at −1.6 eV. As suggested by Xiang *et al.*,[10] we find that the width of the acceptor states (unoccupied portion of the valence bands), containing one hole per supercell, depends on x up to a certain value. Note that the unoccupied part of $N(E)$ is essentially the same in the (1,1,4) and (1,1,5) supercells.

IV. DISORDERED BORON (CPA)

Now we describe CPA calculations which explicitly treat randomly distributed B substitutionals with concentration x.

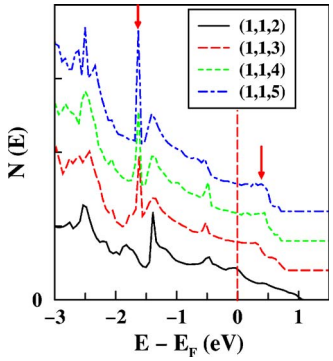

FIG. 5. (Color online) Total DOS of the $(1,1,m)$ cube supercells (m=2,3,4,5); in each case there is one hole per supercell unoccupied. The arrows denote peaks with strong B character. The Fermi energies of every plot are set to zero and spacing of each plot in the y axis is chosen as 2 states/eV.

We calculate x=0.005=1/200 to approximate an isolated boron, and x=0.025 very close to the optimal superconducting concentration c_B. The CPA spectral density for x=0.025, rendered as a "smeared" band structure, is displayed in the full band region in Fig. 6. The bands are like those from the virtual crystal approximation used earlier[7,8] except that lifetime effects (appearing as a broadening) are visible. The effect of disorder is strongest in the conduction (unoccupied) band near 17 eV. The valence (occupied) band is less affected. Even for only 2.5% B doping, the disordered broading is clearly visible in the doubly degenerate band near E_F along Γ-*L*, and near −12 eV along the *X*-*W* line. The former comes from mixing with B $2p$ states and the latter has more admixture of B $2s$ states. It is of course no accident that the disorder broadening resulting from the CPA treatment is largest in the valence band (in the zero to −2 eV region relative to E_F) where the B-derived band shifts are largest. The broadening arises because the quantum mechanical averaging of the wave function over the atomic potentials becomes less systematic in energy regions where the atomic potentials differ more. In this case a single well-defined band persists but with larger broadening. In strong scattering systems (which it turns out this is not), split-band behavior can result.

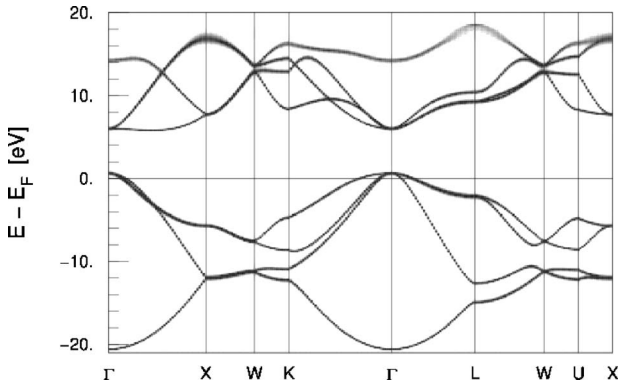

FIG. 6. CPA spectral density, as a "smeared" band structure, in the full valence-conduction band region for x=0.025. The conduction bands around 17 eV are most strongly affected by the chemical disorder, while the valence bands are less affected.

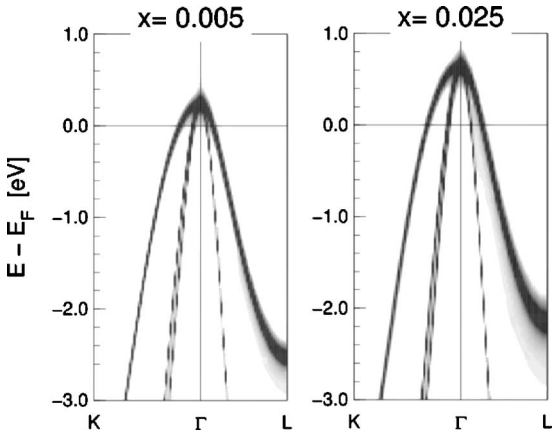

FIG. 7. Blowup CPA spectral density, with Fermi levels aligned, near E_F along the K-Γ-L line for x=0.005 and 0.025. As x increases, E_F is lowered and the disordered broadening increases. The spectral density shows the broadening most clearly at the Γ and L points.

Because the behavior near E_F is important for (super)conductivity, the blowup of the spectral densities near E_F along the K-Γ-L line for x=0.005 and 0.025 are given in Fig. 7. Increasing the B content (x) increases the chemical disorder broadening, in addition to lowering E_F. The change of the disorder broadening at the Γ point is different from that of the L point, because the main B $2p$ character is located just below −2 eV at x=0.025. (See below.) As a result, the broadening at the Γ point is half of that at the L point at x =0.025, while the width at the Γ point is 10% wider than at the L point at x=0.005. Thus disorder broadening effects (such as the residual resistivity) will be nonlinear in x in this region.

The atom-projected B and C DOS from CPA at x=0.025 is shown in Fig. 8. The DOS is similar to those from supercell calculations, but without sharp peaks in the range of −2 eV and 0 eV that arise due to the periodic array of dopant B atoms. The B DOS has a peak at −2 eV and decreases asymmetrically. The C DOS is hardly distinguishable from that of the bulk C. The weight of the B DOS is closer to E_F than that of the C DOS, as in the supercells. Near E_F, the DOS of B is 1.7 times larger than the DOS of C, which indicates the B influence on metallic properties of $C_{1-x}B_x$ is

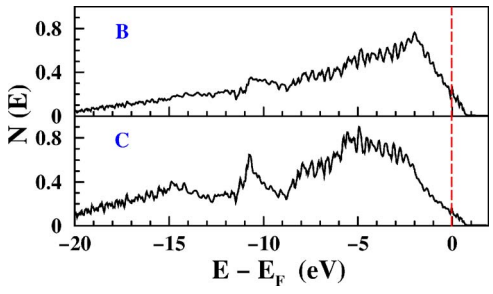

FIG. 8. (Color online) Atom-projected DOS at x=0.025 from the CPA calculation. The picture that results is very similar to that from the supercell calculations. The main peak of B is located at −2 eV, while that of C lies at higher binding energy and is almost identical to that of the bulk C.

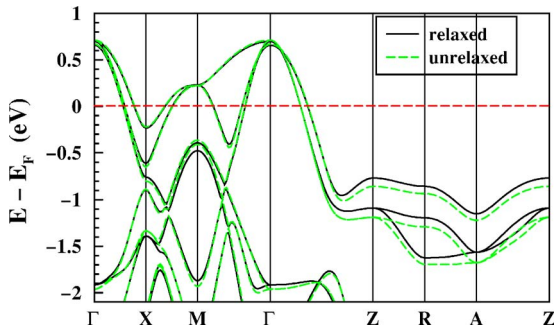

FIG. 9. (Color online) Relaxed and unrelaxed band structures of the B-doped diamond for the $2\times2\times1$ supercell. The relaxation shows little effect. As expected, the strongly hybridized bands between the B and *nn* C on the $k_z=\pi/a$ plane are most affected by the relaxation. The difference between the Fermi energies is 25 meV.

greater than that of an average C atom (but by less than a factor of 2), consistent with measurement by soft X-ray absorption and emission spectroscopy.[26]

V. RELAXATION

Reports of the B-C bond length, when allowed to relax, differ. The 10% value reported in the cluster calculation of Mainwood[17] is clearly unrealistically large. Sitch *et al.*, using a realistic (but not first principles) method with large supercell (216 atoms) found a 4% lengthening,[19] while Blase *et al.*, using first-principles methods but only a 54-atom supercell, reported only a 2% elongation.[9] These values are with respect to the C-C bond length of 1.54 Å for intrinsic diamond. The relaxed and unrelaxed band structures of the B-doped diamond for the $2\times2\times1$ supercell given in Fig. 9 show that the effect of the 2% elongated B-C bond length is to further raise the B-derived bands, i.e., increase the separation from the bulk C bands, although the effect is not major (a maximum of 60 meV). The region between −1.7 and −0.7 eV on the $k_z=\pi/a$ plane of this supercell is most strongest affected, as expected, since that is the region in which B $2p$ states are strongly mixed with *nn* C $2p$ states. This 2% relaxation results in a small (3%) increase in the Fermi energy (by 25 meV), which can be considered as a slight increase in the effective mass. The magnitude of these shifts suggests that relaxation will change numerical results by a few percent but will not change significantly any of the general features of B doping that are discussed above.

VI. SUMMARY

In this paper we have studied the boron spectral density relative to that of C, and quantified to some extent the disorder broadening, in B-doped diamond, using a combination of supercell and random disorder (CPA) approaches. All experimental results that we are aware of support the prevailing viewpoint that this system is a heavily doped degenerate (metallic) semiconductor at the concentration range where superconductivity has been seen, and our studies lie only within this scenario. As far as the average distribution of B character in the itinerant band system is concerned, the CPA

and supercell results are similar. In the region of interest (around the Fermi level for reported levels of doping, not exceeding 5%), the CPA result is that the fraction of B character is 1.7 times that of a C atom. Supercell results are consistent with this value, at least if a little energy averaging is considered.

In the energy-momentum distribution of B character, however, the periodicity in the supercells leads to regions where a band has a much larger fraction of B character than $1.7x$ (the fraction of B character in B_xC_{1-x} given by the CPA), and is split away from bands that are primarily C in character. This effect arises in both the smaller and the larger supercells (3% doping down to 0.8%). The CPA method, on the other hand, leads to bands much like those of intrinsic diamond but disorder broadened to some extent, and with a B content that varies smoothly along the band (that is, with energy and with momentum). The CPA description is buttressed by ARPES data,[15] where mapping of the bands results in diamondlike band topology as occurs in the VCA or (accounting for disorder) CPA.

An attractive feature of the supercell method is its ability to investigate the local environment of the dopant atom, including lattice relaxations. While the cluster CPA method makes it possible within a disordered system, there is very little experience with this capability. The ability to relax atomic positions was used by Blase *et al.*,[9] who obtained a 2% longer B-C bond length than that of diamond; this elongation will lead in turn to a change in the B-C force constant. Whether this factor can account for the difference in spectral distributions obtained by the two supercell methods[9,10] is yet to be resolved.

ACKNOWLEDGMENTS

We acknowledge K. Koepernik for important technical advice. This work was supported by National Science Foundation Grant No. DMR-0421810.

[1] E. A. Ekimov, V. A. Sidorov, E. D. Bauer, N. N. Mel'nik, N. J. Curro, J. D. Thompson, and S. M. Stishov, Nature (London) **428**, 542 (2004).
[2] Y. Takano, M. Nagao, K. Kobayashi, H. Umezawa, I. Sakaguchi, M. Tachiki, T. Hatano, and H. Kawarada, Appl. Phys. Lett. **85**, 2581 (2004).
[3] E. Bustarret, J. Kačmarčik, C. Marcenat, E. Gheeraert, C. Cytermann, J. Marcus, and T. Klein, Phys. Rev. Lett. **93**, 237005 (2004).
[4] V. A. Sidorov, E. A. Ekimov, S. M. Stishov, E. D. Bauer, and J. D. Thompson, Phys. Rev. B **71**, 060502(R) (2005).
[5] H. Umezawa, T. Takenouchi, Y. Takano, K. Kobayashi, M. Nagao, I. Sakaguchi, M. Tachiki, T. Hatano, G. Zhong, M. Tachiki, and H. Kawarada, cond-mat/0503303 (unpublished).
[6] Y. Takano, M. Nagao, T. Takenouchi, H. Umezawa, I. Sakaguchi, M. Tachiki, and H. Kawarada, cond-mat/0507476 (unpublished).
[7] L. Boeri, J. Kortus, and O. K. Andersen, Phys. Rev. Lett. **93**, 237002 (2004).
[8] K.-W. Lee and W. E. Pickett, Phys. Rev. Lett. **93**, 237003 (2004).
[9] X. Blase, Ch. Adessi, and D. Connétable, Phys. Rev. Lett. **93**, 237004 (2004).
[10] H. J. Xiang, Z. Li, J. Yang, J. G. Hou, and Q. Zhu, Phys. Rev. B **70**, 212504 (2004).
[11] Y. Ma, J. S. Tse, T. Cui, D. D. Klug, L. Zhang, Y. Xie, Y. Niu, and G. Zou, Phys. Rev. B **72**, 014306 (2005).
[12] M. Cardona, Solid State Commun. **133**, 3 (2005).
[13] Yu. G. Pogorelov and V. M. Loktev, cond-mat/0405040 (unpublished).
[14] G. Baskaran, cond-mat/0404286 (unpublished).
[15] T. Yokoya, T. Nakamura, T. Matsushita, T. Muro, Y. Takano, M. Nagao, T. Takenouchi, H. Kawarada, and T. Oguchi, Nature (London) **438**, 647 (2005).
[16] A. T. Collins and A. W. S. Williams, J. Phys. C **4**, 1789 (1971); for a recent review, see K. Thonke, Semicond. Sci. Technol. **18** S20 (2003).
[17] A. Mainwood, J. Phys. C **12**, 2543 (1979).
[18] A. S. Barnard, S. P. Russo, and I. K. Snook, Philos. Mag. **83**, 1163 (2003).
[19] P. K. Sitch, Th. Köhler, G. Jungnickel, D. Porezag, and Th. Frauenheim, Solid State Commun. **100**, 549 (1996).
[20] K. Koepernik and H. Eschrig, Phys. Rev. B **59**, 1743 (1999).
[21] K. Koepernik, B. Velicky, R. Hayn, and H. Eschrig, Phys. Rev. B **55**, 5717 (1997).
[22] J. A. Blackman, D. M. Esterling, and N. F. Berk, Phys. Rev. B **4**, 2412 (1971).
[23] D. Kasinathan, K.-W. Lee, and W. E. Pickett, Physica C **424**, 116 (2005).
[24] In the unit cell, there are two types of $2n$ C. One is surrounded by two B on the *a*-*b* plane, and another is along the diagonal direction from B. While the former is affected more strongly by the B, the latter acts like the bulk C. So we call only the former $2n$ C in this paper.
[25] J. Nakamura, E. Kabasawa, N. Yamada, Y. Einaga, D. Saito, H. Isshiki, S. Yugo, and R. C. C. Perera, Phys. Rev. B **70**, 245111 (2004).
[26] J. Nakamura, T. Oguchi, N. Yamada, K. Kuroki, K. Okada, Y. Takano, M. Nagao, I. Sakaguchi, H. Kawarada, R. C. C. Perera, and D. L. Ederer, cond-mat/0410144 (unpublished).